Automatic image-based detection and inspection of paper fibres for grasping

Juha Hirvonen and Pasi Kallio

Micro- and Nanosystems Research Group

Department of Automation Science and Engineering

Tampere University of Technology

Tampere, Finland

E-mail: juha.hirvonen@tut.fi

Abstract

This paper presents an automatic computer vision algorithm that detects individual paper fibres from an image, assesses the possibility of grasping the detected fibres with microgrippers, and detects the suitable grasping points. The goal of the algorithm is to enable automatic fibre manipulation for mechanical characterization, which has traditionally been slow manual work. The algorithm classifies the objects in images based on their morphology, and detects the proper grasp points from the individual fibres by applying given geometrical constraints. We test the ability of the algorithm to detect the individual fibres with 35 images containing more than 500 fibres in total. We compare the graspability analysis and the calculated grasp points with the results of an experienced human operator with 15 images that contain a total of almost 200 fibres. The detection results are outstanding, with fewer than 1 percent of fibres missed. The graspability analysis gives sensitivity of 0.83 and specificity of 0.92, and the average distance between the grasp points of the human and the algorithm is 220 µm. Also, the choices made by the algorithm are much more consistent than the human choices.

Keywords: fibres, automatic testing, microrobotics, grasping, image analysis

1. Introduction

Paper fibres are wood cells that are separated from wood, either chemically or mechanically. They are typically 0.8–4.5 mm long and 16–70 µm wide, depending on their type [1]. When the fibres are pressed together with a

force and dried in high temperature, they form a network structure that is paper. Since the fibres are the main component of paper, it is important to understand their mechanical properties in order to understand the mechanical properties of paper. Also, given the increasing recent interest in chemical functionalization of fibres – that is, adding properties such as hydrophobicity by chemical treatment [2] – interest in fibre-level testing has also grown.

The traditional methods for fibre research are slow and laborious. They require an experienced operator and consist of manual work phases that demand high precision and dexterity. Microrobotics has been effectively applied in manipulation of the micro-scale objects such as biological cells [3], carbon nanotubes [4] and parts in microassembly [5], which makes it an extremely promising tool for fibre studies as well.

Existing studies have proven the functionality and the benefits of the microrobotic approaches in fibre studies [6-8]. However, the systems have to be automated in order to unleash their full potential. Currently, the platforms require a skilled operator and the yield is too low for the results to be statistically significant. Vision-based automation is the most suitable method for this problem. Among the main challenges are distinguishing the most suitable fibres for grasping and detecting the proper fibre sections to grasp. Also, common fibre parameters such as length and curl should be calculated from the graspable fibres. In a typical set-up, the location and the orientation of the fibres are random. Some fibres are too curly for grasping, while others are too short for the measurements. Some fibres are too close to each other for grasping, and some fibres become entangled with each other. These are all factors that need to be considered.

A number of papers have been published in recent years about computer vision algorithms for fibre studies. The reported studies include methods for industrial fibres [9, 10], textile fibres [11–14] and paper fibres [15–17].

Shin et al. [9] presented a method for measuring the diameter of electro-spun fibres, utilizing SEM images of fibre networks. Wan et al. [10] discussed automatic segmentation of microscope images of cross-sections of cut and resin-embedded fibre sections.

Yang et al. [14] reported a method for detecting foreign fibres (plastic, hairs, remnants of binding ropes, etc.) mixed in cotton to ensure the quality of the final product. Ikiz et al. [11] described a method of measuring the

length of cotton fibres. Adel et al. [13] presented a method for defining goodness measures such as maturity index, circularity index, and fineness for cotton, as well as a simple strategy for distinguishing minimally overlapping fibres. Wang [12] discussed an algorithm with which the length and maturation index of cotton fibres is measured. This method involves a strategy to classify some of overlapping fibres to intra-fibre and inter-fibre cross-overs by utilizing the form of the intersection. In all of the above-mentioned papers, the fibre samples are trapped between glass slides [11, 13] or a scanner [12]. In maturation index calculation, fibres are cut to smaller segments [12, 13].

Hirn et al. [15] compared commercial paper fibre analysers. These analysers are based on high-speed cameras and narrow flow cells, in which the fibres flow in suspension. The analysers measure fibre morphological parameters such as length, curl, fine content, and fibrillation. Eckhart et al. [16] presented a flow-cell-based fibre flexibility measurement in which the fibre is deformed by liquid flows and the deformation is measured by a camera. Axelsson et al. [17] discussed a method for tracking fibres in 3D in X-ray microtomography images of paper.

As the above summary shows, research has been conducted into the morphological properties of fibres. However, none of the presented techniques is fully applicable to the problem presented in this paper. Some of those studies discuss analysis of segments of fibres [9, 12, 13], and some techniques are fully based on segments of fibres [10, 17]. A sole fibre detection technique is presented in [14]. The experiment design ensures that there are no multiple fibres in images [11, 15, 16]. The methodology for segmenting fibre and estimating its centreline for calculation of length is presented in [11–13, 16], but those algorithms lack the further analysis of the fibre geometry that is essential for grasping.

This paper presents an image-based method for detection and inspection of individual paper fibres for microrobotic manipulation. The fibre samples and the imaging hardware are presented in Section 2. The proposed computer vision algorithm is described in Section 3 and the experiments and results are discussed in Section 4. The final section offers the conclusions.

2. Test bench and samples

2.1 Microrobotic test bench

Our research group has developed a microrobotic platform for handling and mechanical testing of individual paper fibres [6]. The platform enables direct fibre-level manipulation and measurements and has been used, for example, for measuring fibre flexibility. The platform is composed of a sample stage, microgrippers, and a force sensor. The sample stage comprises a sample holder into which the fibres are placed, a custom-made illumination module that is presented in the following section, and an xy-table and a rotary table to move the fibres close to and align them with the grippers. The sample holder and the illumination module are fixed on the top of the rotary table, and the holder has a 100 µm deep well. The fibres are mixed with water to keep them wet for the flexibility tests, while the purpose of the well is to keep the water layer thin enough that the fibres remain practically in one level. The microgrippers consist of gripper actuators that are attached to 3-DOF micropositioners, and they are used to grasp the fibres and move them towards the force sensor for the measurements. A camera equipped with microscope optics is located on top of the platform for visual feedback. As the wet fibres stay in one level in the sample holder, the top view provides enough spatial information. The devices are operated by a tailored user interface. Fig. 1 presents the platform and Fig. 2 shows the typical grasping procedure.

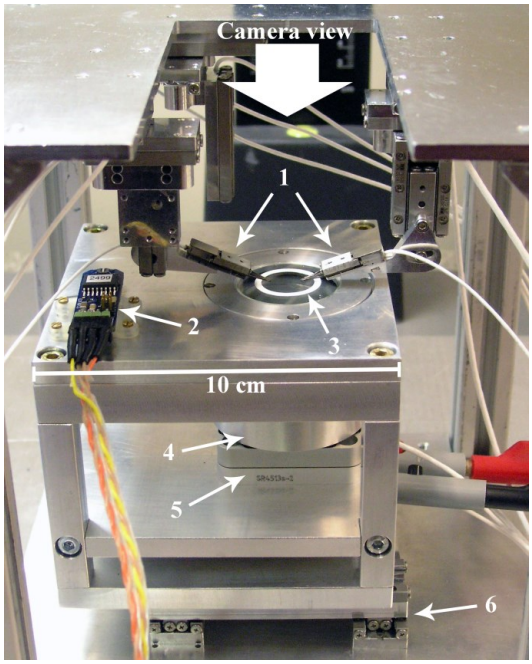

Fig. 1 *The microrobotic platform. 3-DOF microgrippers (1), force sensor (2), sample holder (3), illumination module (4), rotary stage (5), and xy stage (6).*

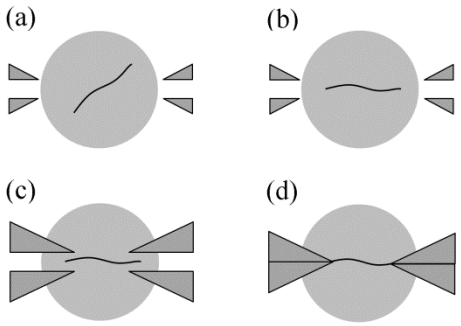

Fig. 2 *Steps of the grasping procedure. Initial position (a), aligning the fibre with the grippers (a), moving the grippers next to the grasping points (c), and grasping the fibre (d).*

2.2 Image acquisition

We utilized polarised backlight in imaging to maximize the contrast between the fibres and the background. We designed and manufactured a special illumination module for this and integrated it with the rotary table of the platform. The sample holder is made of laboratory glass and a plastic ring-shaped sticker with a 16 mm inner diameter and 100 µm thickness is fixed on the glass to generate a shallow well for the wet fibre samples. The light source is situated beneath the sample holder. There is one polariser between the light source and the sample holder and another polariser between the sample holder and the camera. When the angle between the polarisers is 90°, only the light going through the fibre samples or the plastic ring passes the second polariser and travels to the camera. The illumination unit is presented in more detail in [18].

The camera in the setup was an AVT Manta G504b monochrome camera, and the images had resolution of 2452 x 2056 and depth of 8 bits. The optics was a Navitar 12x motorized zoom. We used the software provided by the camera manufacturer for image acquisition.

2.3 Fibre samples

We prepared the fibre samples from unbleached softwood kraft pulp. We mixed small amounts of pulp with distilled water to acquire fibre solutions with different concentrations. Here, 20 mg of pulp was mixed with 20 ml, 15 ml, 10 ml, and 8 ml of water. Pipette is used in dosing fibre suspension onto the sample holder of the test bench, and we obtained test images with different fibre densities by using different concentrations.

3. Algorithm for fibre detection and inspection

The proposed machine vision algorithm automatically detects fibres suitable for grasping from the image. The algorithm has two steps: fibre detection and fibre inspection. The goal of the fibre detection step is to extract the foreground containing the plastic ring, fibres, and trash within the samples from the background, and to further extract the fibres from the ring and the trash. In the fibre inspection step, the objects describing fibres are inspected one by one and classified either as graspable or non-graspable. Some common parameters describing the fibre morphology are then calculated for the graspable fibres. We implemented the algorithm in Python using the modules OpenCV [19] and NumPy [20].

3.1 Fibre detection

A binary image is produced to extract the foreground and background. The contrast between the background and foreground is high due to the illumination method, and therefore we apply global thresholding in binarisation. The imaging conditions are controlled, which means that the same fixed threshold value is suitable for all of the experiments. We use a moderately low threshold value T to minimize the cracks generated to the fibres and to make the plastic ring visible. Consequently, we have white objects describing the ring, the fibres, and the trash on a black background.

The first task after thresholding is to detect the plastic ring. The ring creates the boundaries of the area and the fibres that are very close to the ring should not be grasped in order to avoid collisions between the grippers and the ring. The ring is always the largest binary object in the image, due to its geometry. Accordingly, the ring is detected by detecting all the 8-connected binary objects (blobs) in the image and selecting the one with the highest number of pixels. The innermost border of this blob describes the innermost border of the ring, thereby creating the boundaries. If fibres are in contact with the ring, they are part of the boundary. This is valid since those fibres are too difficult to be grasped.

We obtain the blobs describing the fibres and trash by masking the binary image with a mask generated from the ring borders. Since the length range (L_{min}, L_{max}) of the fibres is known, we remove the trash by omitting all the blobs with a diameter shorter than the minimum fibre length L_{min} in the experiment. The remaining blobs are morphologically closed to smooth their edges. Now, only the blobs describing the fibres are in the image, and

we detect those that are sufficient for grasping by inspecting their morphology. The blobs with a diameter longer than L_{max} have to be comprised of multiple fibres and do not need to be taken for further inspection.

3.2 Fibre inspection

In this step, the blobs that resulted in the fibre detection step are inspected individually. The fibres sufficient for grasping should fulfil three conditions. First, they should not be overlapping with other fibres. It is very difficult to distinguish the order and the parts of the overlapping fibres. Some simple special cases regarding the parts were solved in the reviewed literature [13, 14], but these works do not detect the order, which is crucial in grasping. However, fibres are cheap testing material, which means there is no need to be able to process all the fibres on the sample holder. The second condition is that the fibre should be sufficiently straight. Curvy fibre parts jump from or get entangled between the gripper jaws. Finally, there should be enough space around the fibre to enable the grasping.

To detect the overlapping and be able to analyse the curliness of the fibre, the object is thinned to one pixel wide. We use the thinning method described in [14], as it has been widely used in similar problems [15, 16]. Thinning may create some unwanted spurs in the uneven and curvy sections of the objects. The pruning method presented in [15] is applied to remove these spurs. It is an iterative algorithm consisting of two primary steps. In the first step, the end points and the branch points of the skeleton are detected by applying the hit-and-miss procedure and the suitable 3 x 3 kernels. In the second step, the skeleton sections between an end point and a branch point shorter than a given maximum spur length λ are removed. These two steps are repeated until no change occurs in the skeleton. This way, branched spurs are removed as well. After pruning, all the remaining branch points are fibre cross-over points. These branch points are detected, and all the objects that have branch points are classified as non-graspable. Fig. 3 presents the process of thinning, pruning and branch point detection.

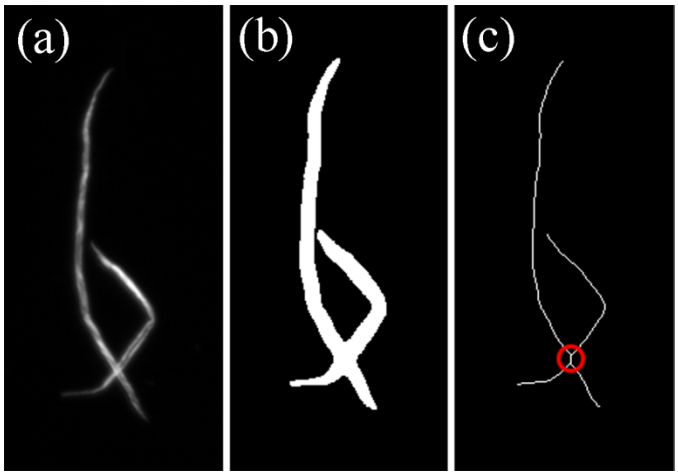

Fig. 3 *Thinning, pruning and detecting branch points. Original image (a), binary image (b), and thinned and pruned image with the branch points encircled (c).*

Now, all the fibre skeleton objects in the binary image represent an individual fibre. Next, the skeleton objects are inspected individually. The surroundings of the fibre should be free of other objects to enable grasping. Therefore, the distance between the closest object point and the skeleton should be at least d_{min}. If no objects are closer, the suitable grasping points are searched from the skeleton. The following four conditions should be met (as visualized in Fig. 4).

I. The fibre section close to the grasping point should be straight enough to fit in between the gripper jaws. Thus, if the grasp points are connected with a straight line, the angles between this line and the lines connecting the grasp point to the end points of its section should be $\geq \alpha_{min}$ (the section end point between the grasp point and the fibre end point) and $\leq 180^\circ - \alpha_{min}$ (the section end point between the grasp points). The gripper geometry defines the section length e_{min}. This is clarified later in this paper.

II. The ending of the fibre should not be folded double on the grasping point. Thus, a line connecting the grasp points and the lines connecting the grasp points to the nearest fibre end points should have angle $> 90^\circ$.

III. The length of the fibre section between the grasping points L' should exceed the minimum length $l_{\min}$ required for the further experiments.

IV. The length of the endings e_1, e_2 should be in a given range $[e_{min}, e_{max}]$.

Condition I depends on the gripper geometry but Condition III and the parameter e_{max} in Condition IV are user-given parameters and are highly dependent on the experiments to be performed. The angle calculation in

Conditions I and II is based on the fact that the fibre must be aligned with the grippers before grasping. Therefore, the straight line connecting the grasp points defines the axis of the grippers.

Now, the binary image consists of m skeleton objects that are defined as

$$S_k(i) = [u_k(i), v_k(i)], \quad k = 1..m, \quad i = 1..n, \tag{1}$$

where n is the number of pixels in the skeleton, and $u_k(i)$ and $v_k(i)$ are the horizontal and vertical coordinates of the ith pixel of the skeleton S_k, respectively.

The algorithm inspects the four conditions on each skeleton object. It involves the following six steps:

1) Select the leftmost upmost non-inspected fibre skeleton object $S_k(i)$.
2) Calculate the length array $L(i)$, stating the cumulative length of the fibre in each of its points from the skeleton as in [11, 21]. If $L(n) < l_{min} + 2*e_{min}$, go to Step 1 (Conditions III and IV).
3) Form pairs of grasp point candidates $S_k(a)$ and $S_k(b)$. Use as initial values for a and b values that satisfy $L(a) > e_{min}$, $L(n) - L(b) > e_{min}$. Go through the point combinations by increasing a or decreasing b until $L(a) > e_{max}$ OR $L(n) - L(b) > e_{max}$ OR $L(b) - L(a) < l_{min}$ (Conditions III and IV). All the grasping point pairs that fulfill the following conditions are candidates for the final grasping points.
    a. Find points $S_k(a^-)$, $S_k(a^+)$ that satisfy $L(a) - L(a^-) = e_{min}/2$, $L(a^+) - L(a) = e_{min}/2$, and points $S_k(b^-)$, $S_k(b^+)$ that satisfy $L(b) - L(b^-) = e_{min}/2$, $L(b^+) - L(b) = e_{min}/2$. Let us denote the points $S_k(a^-)$, $S_k(a)$ and $S_k(a^+)$ as A, B and C and the points $S_k(b^-)$, $S_k(b)$ and $S_k(b^+)$ as D, E and F, respectively. Then, $\angle$ABE, $\angle$BEF $\geq \alpha_{min}$ and $\angle$EBC, $\angle$BED $\leq 180° - \alpha_{min}$ (Condition I). See Fig. 4.
    b. Let us denote the fibre endpoints $S(1)$ and $S(n)$ as O and Y. Then, $\angle$OBE, $\angle$BEY $> 90°$ (Condition II). See Fig. 4.

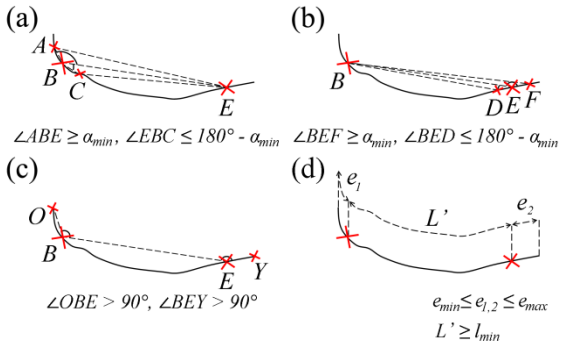

Fig. 4 *Grasping rules. The straightness constraints (a, b, c) and the length constraints (d).*

If no points fulfil the conditions, go to Step 1.

4) The final grasping point pair is that with the longest fibre section between the points. Mark the fibre graspable and save the grasping points.

5) If there are non-inspected fibre objects, go to Step 1.

Fig. 5 shows all the phases of the procedure. Fibre length and curl, which are commonly used parameters for paper fibre [15], are then saved for the graspable fibres. These parameters are important information for the later tests since they have been shown to affect the quality of paper [22]. The fibre length *L(n)* was calculated in Step 2. The curl is calculated as in [23] using the following equation:

$$Curl = \frac{L(n)}{F_{max}} - 1 \quad , \tag{2}$$

where F_{max} is the distance between the points in the fibre that are furthest apart. F_{max} is calculated as the longest side of a rotated minimum area bounding box drawn around the fibre blob.

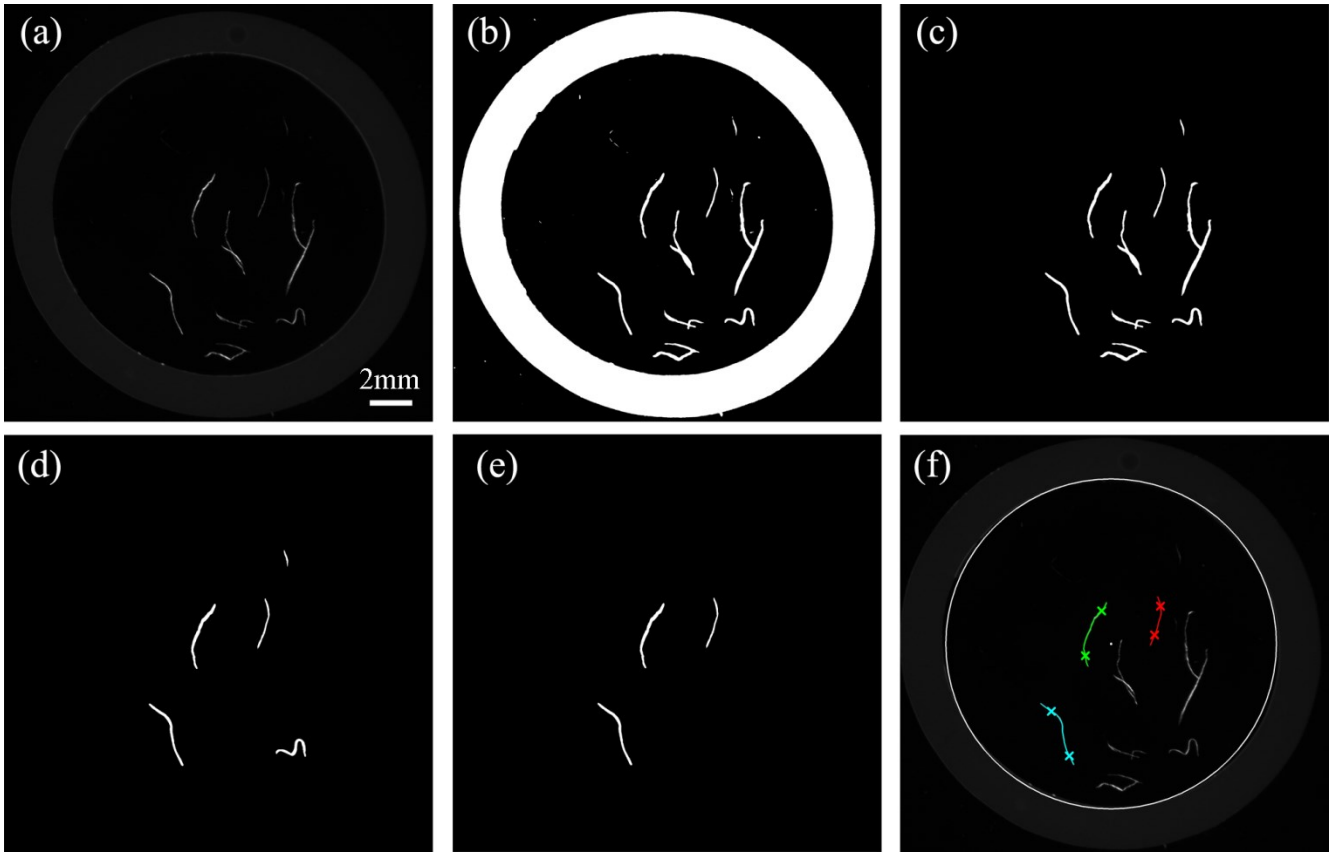

Fig. 5 *Original image (a), binary image (b), the ring and trash removed (c), overlapping fibres removed (d), graspable fibres (e), and centrelines, grasping points and the inner border of the plastic ring marked on the original image with different colours (f).*

4. Experiments and results

We tested the algorithm by taking 35 images of between four and 55 fibres. The total number of fibres imaged was 562. We injected the fibre solution to the sample holder with a pipette, which meant that the orientation and number of the fibres was totally random. We used the images to assess the performance of the algorithm, and divided the assessment into two parts. First, we investigated the pre-processing steps; that is, the steps that detect individual fibres from the original image. This includes fibre detection and early phases of fibre inspection. We then studied the graspability analysis, comprising the decision regarding whether the fibre is graspable or not and the search of the grasp points. We utilized an experienced human operator in this phase.

4.1 Assessment of pre-processing

We used five images as a teaching group to find an appropriate threshold T and maximum spur length λ, and the remaining 30 images as the testing group for the algorithm. There were 134 and 428 fibres in the teaching group and the testing group, respectively. The parameters are seen in Table 1. We assessed fibre detection and overlapping detection by calculating goodness measures.

Table 1 The parameters for pre-processing

Parameter	Explanation	Value
T	Threshold for binarisation	12
L_{min}	Minimum fibre length	1.0 mm
L_{max}	Maximum fibre length	4.0 mm
Λ	Maximum spur length	0.10 mm

We calculated the probability of missing a fibre, fusing together multiple fibres close to each other, and generating cuts to a fibre for the fibre detection step. In addition, we calculated the probability of generating the cut in the close proximity of the fibre end since these kinds of cuts do not change the fibre geometry significantly.

We assessed the overlapping detection by calculating its sensitivity and specificity, which are defined as follows.

$$sensitivity = \frac{TP}{TP + FN} \tag{3}$$

$$specificity = \frac{TN}{TN + FP}, \tag{4}$$

where TP is the number of true positives, TF is the number of false positives, TN is the number of true negatives and FN is the number of false negatives. We counted true positives, false positives, true negatives and false negatives from the images manually. Table 2 shows the goodness measures.

Table 2 The goodness measures of the pre-processing steps

Fibre detection			
Not detected %	Cut %	Cut in the tip %	Fused %
0.3	8.5	5.3	0.5
Overlapping detection			
Sensitivity		Specificity	
0.80		1.00	

The errors in fibre detection are usually caused by fibre parts that are either narrow or twisted parallel to the camera or both. These parts tend to be cut in thresholding. These parts are often in the end sections of the fibres, as can be seen in the table.

The most problematic cases for the overlapping detection were almost parallel fibres entangled together and short overlapping fibres. Then, the lengths of the crossing fibre sections were often shorter than the given maximum spur length λ and were therefore removed in pruning. However, false positives did not occur at all, although it could be questioned whether very short fibre pieces over longer ones would cause problems in grasping and if they should therefore be identified as overlapping fibre.

4.2 Assessment of graspability analysis

We compared the performance of the algorithm with the choices of an experienced human operator (six years of experience in microrobotic manipulation of fibres). We used 10 images as a test group for choosing the parameters l_{min}, e_{min}, e_{max}, d_{min} and α_{min}. The human operator selected the grasping points by clicking them with a mouse using a simple user interface. The parameters of the algorithm were adjusted to acquire grasping points that were as similar as possible to those selected by the human. The grasping parameters are shown in Table 3.

Table 3 The parameters for grasping

Parameter	Explanation	Value
d_{min}	Minimum distance between the fibre and the closest object	0.50 mm
l_{min}	Minimum length of the fibre between the grippers	0.75 mm
e_{min}	Minimum ending length	0.50 mm
e_{max}	Maximum ending length	1.50 mm
α_{min}	Minimum angle within the fibre section to be grasped	145˚

We then assessed the performance of the algorithm using the found parameters against the human operator. We studied the similarity between the fibres classified as graspable and the distance between the grasping points. In both studies, we compared the human and the algorithm choices with themselves and with each other to observe the consistency and the uniformity of the choices. In this experiment, we used 15 images, each with between four and 23 fibre objects, for a total of 189 fibre objects. We created four sets of the images, in which all the images were in different orders and the orientations of 0˚, 90˚ 180˚ and 270˚. The operator processed the sets during different weeks without knowing that the sets contain the rotated versions of the same images. This made it possible to measure the consistency of the choices. The grasping point search algorithm is based on skeletonization, which is sensitive to changes in the binary image. Thus, the orientation changes of the imaged scene that occur due to the rotary table turns needed for fibre alignment (see Fig. 2) may cause changes in the detected grasping point and in the entire graspability analysis. Therefore, it is essential to also measure the consistency of the results of the algorithm with different rotations. Here, we simulate the rotary table turns by rotating the images.

We calculated confidence levels for the fibres classified as graspable in order to provide a numerical result for the consistency. The confidence level is defined as the relationship between the number of images in which the same fibre object is classified as graspable and the total number of the images in which the fibre object appears. In the example in Fig. 6, Fibre A has been classified as graspable in all orientations except for 90˚, while Fibre

B has been classified as graspable in all the orientations. This gives Fibre A and Fibre B the confidence levels of 0.75 and 1.00, respectively. We calculated the confidence levels for each fibre that was classified as graspable at least once and generated a histogram of the results. The high count in the confidence level 1.00 indicates high consistency and the high count in the confidence level 0.25 indicates low consistency. The histogram is seen in Fig. 7.

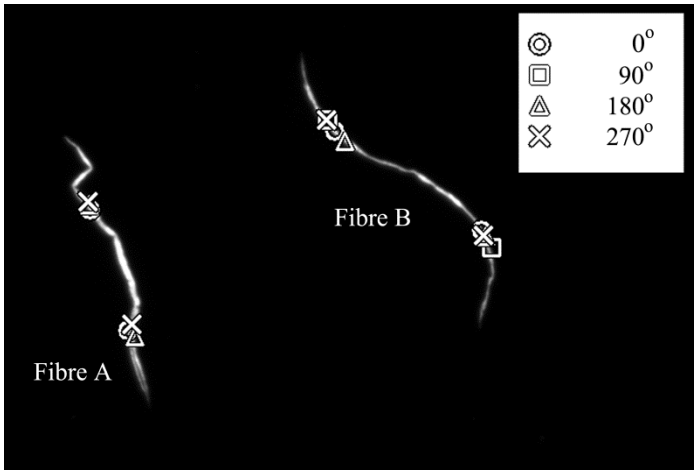

Fig. 6 *Grasping points for two fibres in four orientations rotated back to the 0˚ orientation.*

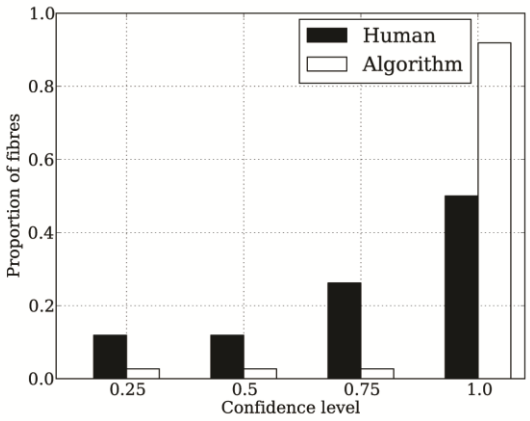

Fig. 7 *Histogram of the confidence levels. Total numbers of the fibres classified as graspable by the human and the algorithm were 45 and 36, respectively.*

As shown in Fig. 7, the algorithm is far more consistent with its choices than the human, with over 90 percent of the graspable fibres having a confidence level of 1.00. Only two fibres have a confidence level of 0.75 and one had a level of 0.50. This means that some rare borderline cases are not detected as graspable in all the orientations.

We calculated the mean distance between the grasping points of the same end of the fibre in different orientations, with the results presented in Table 4. We also calculated the average execution time of the algorithm per image and compared it with the average time required for the human operator to make the choices per image. These times are seen in Table 5.

Table 4 The mean distances between the grasping points of the same fibre

	Mean distance (μm)
Human – human	130 ± 55
Algorithm – algorithm	65 ± 40
Human – algorithm	220 ± 90

Table 5 The average execution times of the algorithm and the human operator per image

	Execution time (s)
Human	18.4
Algorithm	4.2

As the length of the fibres varies between 1.0 mm and 4.0 mm and one pixel corresponds to 11 μm, the distances are relatively low. The average distance between the grasping points detected by the algorithm is half of the corresponding result of the human. Thus, the detected grasping points are also more consistent than the human's choices. However, the average distance between the grasping points selected by the algorithm and those selected by the human is the largest. This implies that there are some differences in the selection criteria. The most notable differences were in long curly fibres and long fibres that have sharp angles. In those cases, the maximum angle and the maximum ending length constraints collided with the human decision making. Nevertheless, the distances are tolerable in the scale of the fibres. Also, the execution time of the algorithm is less than 25 % of the time required for the experienced human operator to make the choices.

Finally, we calculated sensitivity and specificity for the algorithm. Here, the true positives were the fibres that both the human operator and the algorithm classified as graspable, and the true negatives were the fibres that both classified as non-graspable. Table 6 presents the results and shows that the algorithm imitates the human choices fairly well. The sensitivity is lower than the specificity, which indicates lower ability to detect a graspable fibre than to exclude a non-graspable one. However, the low consistency of the human choices affects these measures.

Table 6 The goodness measures of the graspability analysis

Sensitivity	0.83
Specificity	0.92

5. Conclusion

This paper has presented a computer-vision-based method for selecting fibre samples for grasping in a microrobotic system. The system consists of grippers with three linear axes and a sample stage capable of rotation and 2D translation. As this is a popular configuration in microrobotics, and especially in fibre research, the method is widely applicable. The algorithm comprises steps for detecting all the fibre objects in the image and inspecting the graspability of each individual fibre object. This is important since it is very difficult to affect the initial location and orientation of the fibre samples in the sample holder, and there is often trash mixed in the samples. The outcome of the algorithm is a classification of whether the fibre is graspable or not and the image coordinates for the actuators to grasp. The image coordinates can be transformed to the manipulator positions after calibrating the actuators. As the fibres are inside a thin layer of water, the 2D coordinates offer enough spatial information for grasping.

The excellent results gained in the fibre detection step indicate that the probability of missing a fibre or obtaining invalid morphologic information either by interpreting one fibre as multiple fibres or adjacent fibres as overlapping fibres are very low. This provides the reliability required in automation. The rather high sensitivity (0.83) and specificity (0.92) yielded in the graspability analysis show that the formulated grasping rules match quite well with the procedures of an experienced human operator. The relatively low distance (220 μm) between the grasping points selected by the human and the algorithm implies the same. Also, the algorithm was more

consistent and remarkably faster than the human operator in both tasks. The results presented in this paper confirm that the proposed algorithm can be reliably used in automated fibre handling operations for identifying graspable fibres and selecting the grasping points.

6. Acknowledgments

The financial support from GETA (Graduate School of Electronics, Telecommunications and Automation) and the Academy of Finland (grant numbers 253364 and 256527) is greatly acknowledged. Also, the authors would like to acknowledge MSc Pooya Saketi for his valuable assistance during the experiments.

References

1. Ververis, C., Georghiou, K., Christodoulakis, N., *et al*: 'Fiber dimensions, lignin and cellulose content of various plant materials and their suitability for paper production', Ind. Crops Prod., 2004, **19,** (3), pp. 245–254
2. Lange, C., Lundin, T. and Fardim, P.: 'Hydrophobisation of mechanical pulp fibres with sodium dodecyl sulphate functionalised layered double hydroxide particles', Holzforschung, 2012, **66,** (4), pp. 433–441
3. Inoue, K., Arai, T., Tanikawa, T., *et al*: 'Dexterous micromanipulation supporting cell and tissue engineering'. Proc. International Symposium on Micro-NanoMechatronics and Human Science, Nagoya, Japan, 2005, pp. 197–202
4. Eichhorn, V., Carlson, K., Andersen, K. N., *et al*: 'Nanorobotic manipulation setup for pick-and-place handling and nondestructive characterization of carbon nanotubes'. Proc. IEEE International Conference on Intelligent Robots and Systems, San Diego, USA, 2007, pp. 291–296
5. Probst, M., Hürzeler, C., Borer, R., *et al*: 'A microassembly system for the flexible assembly of hybrid robotic mems devices', Int. J. Optomechatronics, 2009, **3,** (2), pp. 69–90
6. Saketi, P., Treimanis, A., Fardim, P., *et al*: 'Microrobotic platform for manipulation and flexibility measurement of individual paper fibers'. Proc. IEEE International Conference on Intelligent Robots and Systems, Taipei, Taiwan, 2010, pp. 5762–5767

7. Saketi, P., Von Essen, M., Mikczinski, M., *et al*: 'A flexible microrobotic platform for handling microscale specimens of fibrous materials for microscopic studies', J. Microsc., 2012, **248,** (2), pp. 163–171
8. Mikczinski, M., Nguyen, H. X. and Fatikow, S.: 'Assessing transverse fibre properties: Compression and artificial hornification by periodic compression'. Proc. 15th Pulp and Paper Fundamental Research Symposium, Cambridge, UK, 2013, pp. 803–820
9. Shin, E. H., Cho, K. S., Seo, M. H., *et al*: 'Determination of electrospun fiber diameter distributions using image analysis processing', Macromol. Res., 2008, **16,** (4), pp. 314–319
10. Wan, Y., Yao, L. and Xu, B.: 'Automatic segmentation of fiber cross sections by dual thresholding', J. Eng. Fiber and Fabr., 2012, **7,** (1), pp. 114–120
11. Ikiz, Y., Rust, J. P., Jasper, W. J., *et al*: 'Fiber length measurement by image processing', Text. Res. J., 2001, **71,** (10), pp. 905–910
12. Wang, H.: 'Fiber property characterization by image processing', MSc thesis, Texas Tech University, 2007
13. Adel, G., Faten, F. and Radhia, A.: 'Assessing cotton fiber maturity and fineness by image analysis', J. Eng. Fiber Fabr., 2011, **6,** (2), pp. 50–60
14. Yang, W., Li, D., Zhu, L., *et al*: 'A new approach for image processing in foreign fiber detection', Comput. Electron. Agric., 2009, **68,** (1), pp. 68–77
15. Hirn, U. and Bauer, W.: 'Review of image analysis based methods to evaluate fiber properties', Lenzinger Berichte, 2006, **86,** (1), pp. 96–105
16. Eckhart, R., Donoser, M. and Bauer, W.: 'Single fibre flexibility measurement in a flow cell based device'. Proc. 14th Pulp and Paper Fundamental Reseach Symposium, 2009, Oxford, UK, pp. 247–271.
17. Axelsson, M.: '3D tracking of cellulose fibres in volume images'. Proc. IEEE International Conference on Image Processing, 2006, Atlanta, USA, pp. IV309–IV312
18. Hirvonen, J., Hanninen, A. and Kallio, P.: 'Design and implementation of an illumination system for microrobotic paper fiber studies'. Proc. IEEE International Conference On Robotics and Automation, Hong Kong, Hong Kong, 2014, pp. 5854–5859
19. Bradski, G. and Kaehler, A.: 'Learning OpenCV: Computer Vision with the OpenCV Library' CA, USA: (O'Reilly Media, 2008)
20. Oliphant, T. E.: 'Python for scientific computing', Comput. Sci. & Eng., 2007, **9,** (3), pp. 10–20

21. Niemisto, A., Dunmire, V., Yli-Harja, O., *et al*: 'Robust quantification of in vitro angiogenesis through image analysis', IEEE Trans. Med. Imag., 2005, **24,** (4), pp. 549–553.

22. Tiikkaja, E.: 'Application of an optical fibre analyser and a tube flow fractionator to the estimation of quality potential of TMP: Experimental study', PhD thesis, University of Oulu, 2007

23. Page, D., Seth, R., Jordan, B., *et al*: 'Curl, crimps, kinks and microcompressions in pulp fibres – their origin, measurement and significance'. Proc. 8th Pulp and Paper Fundamental Reseach Symposium, Oxford, UK, 1985, pp. 183–227